Chapter Number

Multilayered Structure as a Novel Material for Surface Acoustic Wave Devices: Physical Insight

Natalya Naumenko
Moscow Steel and Alloys Institute (Technological University)
Russia

1. Introduction

Since 70-ies, when the first delay lines and filters employing surface acoustic waves (SAW) were designed and fabricated, the use of SAW devices in special and commercial applications has expanded rapidly and the range of their working parameters was extended significantly (Hashimoto, 2000; Ruppel, 2001, 2002). In the last decade, their wide application in communication systems, cellular phones and base stations, wireless temperature and gas sensors has placed new requirements to SAW devices, such as very high operating frequencies (up to 10 GHz), low insertion loss, about 1 dB, high power durability, stable parameters at high temperatures etc.

The main element of a SAW device is a piezoelectric substrate with an interdigital transducer (IDT) used for generation and detection of SAW in the substrate. The number of single crystals utilized as substrates in SAW devices did not increase substantially since 70-ies because a new material must satisfy the list of strict requirements to be applied in commercial SAW devices: sufficiently strong piezoelectric effect, low or moderate variation of SAW velocity with temperature, low cost of as-grown large size crystals for fabrication of 4-inch wafers, long-term power durability, well developed and non-expensive fabrication process for SAW devices etc. Today only few single crystals are utilized as substrates in SAW devices: lithium niobate, $LiNbO_3$ (LN), lithium tantalate, $LiTaO_3$ (LT), quartz, SiO_2, lithium tetraborate, $Li_2B_4O_7$ (LBO), langasite, $La_3Ga_5SiO_{14}$ (LGS) and some crystals of LGS group (LGT, LGN etc.) with similar properties.

The SAW velocities in these single crystals do not exceed 4000 m/s, which limit the highest operating frequencies of SAW devices by 2.5-3 GHz because of limitations imposed by the line-resolution technology of IDT fabrication. The minimum achievable insertion loss and maximum bandwidth of SAW devices depend on the electromechanical coupling coefficient, which can be evaluated for SAW as $k^2 \approx 2\Delta V/V$, where ΔV is the difference between SAW velocities on free and electrically shorted surfaces. The largest values of k^2 can be obtained in some orientations of LN and LT. Ferroelectric properties of these materials are responsible for a strong piezoelectric effect. As a result, k^2 reaches 5.7% in LN and 1.8% in LT, for SAW. For leaky SAW (LSAW) propagating in rotated Y-cuts of both crystals, the coupling is higher and can exceed 20% for LN and 7% for LT. However, LSAW attenuates because of its leakage into the bulk waves when it propagates along the crystal surface. As a

result, insertion loss of a SAW device increases. Attenuation coefficient depends on a crystal cut and IDT geometry. For example, in 36° to 48° rotated YX cuts of LT and in 41° to 76° YX rotated YX cuts of LN, high electromechanical coupling of LSAW can be combined with low attenuation coefficient via simultaneous optimization of orientation and electrode structure (Naumenko & Abbott, US patents, 2003, 2004). When these substrates are utilized in radiofrequency (RF) SAW filters with resonator-type structures, low insertion loss of 1dB or even less can be obtained. Today such low loss filters are widely used in mobile communication and navigation systems. The main drawback of these devices is high sensitivity of the characteristics to variations of temperature because the typical values of temperature coefficient of frequency (TCF) vary between -30 ppm/°C and -40 ppm/°C for LT and between -60 ppm/°C and -75 ppm/°C for LN.

Contrary to LN and LT, quartz is characterized by excellent temperature stability of SAW characteristics but low electromechanical coupling coefficient, k^2<0.15%. Hence, even in resonator-type SAW filters with very narrow bandwidths, about 0.05%, where the loss of radiated energy is minimized due to the energy storage in a resonator, the best insertion loss achieved in a SAW device with matching circuits is only 2.5-4 dB.

In some orientations of LBO, LGS and other crystals of LGS group, zero TCF is combined with a moderate electromechanical coupling coefficient. However, these crystals have limited applications in commercial SAW devices because low SAW velocities restrict high-frequency applications on LGS and LBO dissolves in water and acid solutions, which prohibits application of conventional wafer fabrication processes to this material and finally results in an increased cost of SAW devices.

Hence, none of available single crystalline materials provides a combination of large piezoelectric coupling, zero TCF and high propagation velocity. A strong need in such material exists today, especially for application in SAW duplexers and multi-standard cellular phones, where the temperature compensation is the key issue because of necessity to divide a limited frequency bandwidth into few channels with no overlapping allowed in a wide range of operating temperatures. As an alternative to conventional SAW substrates, layered or multilayered (stratified) materials were studied extensively since 80-ies but only in the last decade some of these structures found commercial applications in SAW devices, due to the recent successes of thin film deposition technologies and development of robust simulation tools for design of SAW devices on layered structures.

2. Multilayered structures as materials for SAW devices

As described above, the increasing requirements to the substrate materials, on one side, and rapid development of thin film deposition technologies, on the other side, gave rise to the novel class of materials for SAW devices – layered or multilayered structures. One or more films of different materials deposited on a regular substrate can improve its characteristics significantly. A proper combination of a substrate and a thin film helps to overcome the limitations of the conventional SAW substrates. In this section, a brief overview of the layered structures will be given. The examples presented here are currently investigated by different research groups as promising compound SAW substrate materials or found already some applications in SAW devices. The focus is made on the recent achievements in material research mostly motivated by challenges of the rapidly developing market of communication devices. Based on this overview, a generalized multilayered structure,

which includes all described examples, will be derived and a method of investigating this structure will be presented and then applied to few different structures, for which more detailed discussion of SAW propagation characteristics will be given.

The first example of a layered structure is a dielectric isotropic silicon dioxide (SiO_2) film deposited on one of rotated YX-cuts of LN or LT characterized by a high electromechanical coupling. Today these structures attract attention of researchers and SAW designers as the most promising candidates for application in SAW duplexers required in most of popular mobile phone systems (Kovacs et al., 2004; Kadota, 2007; Nakai et al., 2008; Nakanishi et al., 2008]. These RF devices must separate the transmitted and received signals in a narrow frequency interval and in a wide range of operating temperatures, e.g. between -30°C and +85°C. Therefore, substrate materials combining high propagation velocity, high electromechanical coupling and low TCF are strongly required. Due to the opposite signs of TCF in SiO_2 and LT or LN, a layered SiO_2/LT or SiO_2/LN structure allows to obtain the desired combination of characteristics. When it is utilized in a resonator-type filter, the electrodes of IDT and metal gratings are commonly built at the interface between SiO_2 and LN or LT. Besides, a heavy metal, such as copper, is utilized as an electrode material (Nakai et al., 2008). A layered structure with such electrode configuration is schematically presented as *Type 1* in Fig.1. The location of electrodes at the interface helps to keep a high electromechanical coupling and combine it with a large reflection coefficient in SAW resonators. A large metallization thickness effectively reduces resistive losses and results in a high *Q* factor of a SAW resonator. Another advantage of using heavy electrodes is a reduced propagation loss, which is achieved due to the transformation of LSAW into SAW. SAW devices with low insertion loss of 1-2 dB and low TCF of -7ppm/°C, have been successfully realized on such substrates (Kadota, 2007).

A thickness of SiO_2 film in SiO_2/LT and SiO_2/LN structures can vary within a wide range, from a few percent of a SAW wavelength up to a few wavelengths, to provide the required combination of electromechanical coupling, TCF and propagation loss. Moreover, SiO_2 film helps to isolate the working surface of a SAW device from environmental influences and facilitates packaging of SAW chip.

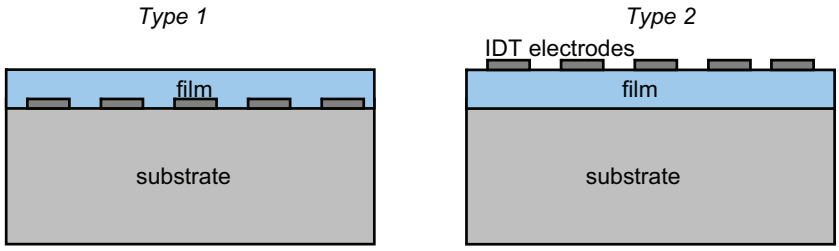

Fig. 1. Two typical structures with one thin film

Another electrode configuration in a structure with one thin film is schematically presented as *Type 2* in Fig. 1, with IDT located on the top surface. It is typical for a piezoelectric film on a non-piezoelectric substrate or on a substrate with low electromechanical coupling coefficient. As a piezoelectric film, zinc oxide ZnO is widely used (Kadota & Minakata, 1998; Nakahata et al., 2000; Emanetoglu et al., 2000; Brizoual et al., 2008). ZnO films are cheap and provide sufficiently high values of electromechanical coupling. The film deposition

technique (e.g. magnetron sputtering) has been well developed for this material. Another piezoelectric film, which is extensively studied as a promising material for high-frequency SAW devices is aluminum nitride (AlN) (Benetti et al., 2005, 2008; Fujii et al., 2008; Omori et al., 2008). It is characterized by chemical stability, mechanical strength, high acoustic velocity and good dielectric quality. Some other piezoelectric films, like CdS or GaN, were investigated previously but did not receive as much attention as ZnO or AlN.

A piezoelectric film is usually combined with silica glass, silicon, sapphire or diamond substrate. Silica glass is cheap, the use of silicon as a wafer enables simple integration of IF and RF components in one chip, sapphire is characterized by high SAW velocities, up to 6000 m/s, and diamond provides the highest SAW velocities among all materials, up to 11000 m/s, and is being used for high frequency SAW devices in the GHz range. For example, SAW resonator with center frequency about 4.5 GHz was built on AlN/diamond structure characterized by SAW velocity about 10000 m/s and $k^2 \approx 1\%$ (Omori et al., 2008). A combination of SAW velocity about 5500 m/s and electromechanical coupling about 0.25% can be obtained in AlN/sapphire structure (Ballandras et al., 2004). To reduce TCF of a SAW device, ZnO film can be combined with quartz or LGS. For example, nearly zero TCF and k^2 about 1.8% was achieved for SAW in ZnO/quartz structure, via optimization of quartz orientation (Kadota et al., 2008).

One more structure, which can be referred to the *Type 1*, recently found application in SAW devices. It is a thin plate of a piezoelectric crystal, such as LN or LT with thickness 10-15 wavelengths, which is directly bonded to a dielectric or semiconductor wafer. The bonding technology (Eda et al., 2000) provides excellent contact between the two materials and allows fabrication of SAW devices with reproducible characteristics on a thin LN or LT plate bonded to a thick silicon or glass wafer. In these structures, high values of electromechanical coupling coefficients typical for LN and LT are combined with improved TCFs, due to low thermal expansion coefficients (TCE) determined by massive silicon, glass or sapphire wafer (Tsutsumi et al., 2004). An example of bonded wafer will be numerically investigated in section 4.

The quality of a contact between LN or LT plate and a silicon wafer can be improved if a thin SiO_2 film is deposited between these materials (Abbott et al., 2005). Such two-layered structure with IDT on the top surface is schematically shown as *Type 3* in Fig. 2. With silicon as a substrate, SiO_2 as the first film and LN or LT as the second film (plate), this structure can give the same advantages as LT/Si or LN/Si bonded wafers but with higher quality contact between the materials. The presence of additional SiO_2 film results in spurious acoustic modes propagating in a SAW device. These modes deteriorate the device performance and should be simulated properly to achieve the desired device characteristics.

Another example of the *Type 3* structure is a silicon wafer with isotropic SiO_2 as the first film and ZnO as the second film. Optimization of SiO_2 and ZnO film thicknesses enables obtaining of a structure with TCF=0 (Emanetoglu et al., 2000). A high frequency SAW device can be built if SiO_2 and ZnO films are deposited atop of a diamond or a sapphire substrate. With ZnO as the first film and isotropic SiO_2 as the second film, the preferential location of IDT electrodes is at the substrate-film interface (*Type 4*). Alternatively, IDT can be built on ZnO surface and then buried in SiO_2 overlay (*Type 5*). For example, Nakahata (Nakahata et al., 2000) reported on a SAW resonator using SiO_2/ZnO/diamond structure with two different electrode configurations (*Type 4* and *Type 5*). Zero TCF, high velocity about 10000 m/s and $k^2 \approx 1.2\%$ were obtained for shear horizontally (SH) polarized SAW mode. A

resonator with center frequency about 2.5 GHz, temperature compensated characteristics and low insertion loss was fabricated on this structure.
Nakahata (Nakahata et al., 1995) reported one more example of the two-layered structure, which can be referred to *Type 4*. It is a ZnO film on a silicon wafer with thin isotropic diamond layer between them. The following SAW characteristics have been obtained: velocity $V \approx 8050$ m/s, $k^2 \approx 1.42$ %, TCF≈0.

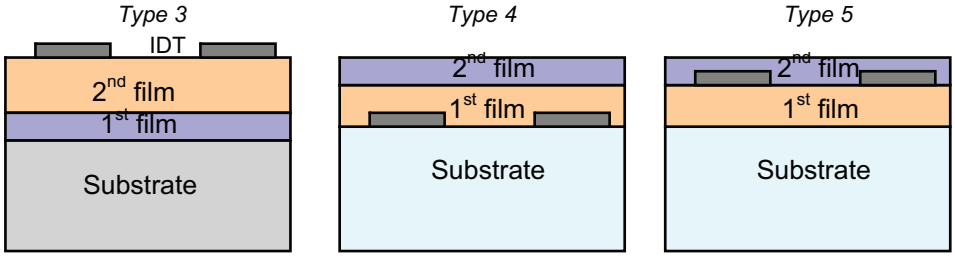

Fig. 2. Three typical structures with two thin films

The examples described above are not aimed at comprehensive survey of layered structures potentially applicable in SAW devices but demonstrate that a variety of layered structures can be referred to a few basic types. A unified approach to analysis of acoustic modes in different layered structures would be beneficial for optimization of SAW devices, because such approach allows comparing characteristics of the same SAW design built on different combinations of film and substrate materials.
The simulation of SAW characteristics is an important part of the SAW device design procedure. In a specified structure, such simulation must take into account orientation of each material if it is anisotropic, film thicknesses, a thickness and shape of IDT electrodes, electrode width to pitch ratio etc. Besides, the accurate analysis of all modes propagating in the investigated structure is required, including the main SAW or LSAW mode and all spurious modes generated by IDT in the specified frequency interval. A number of spurious modes grows with a number of layers and increasing of their thicknesses, which makes the simulation procedure more complicated. Moreover, with increasing film thickness SAW changes its nature and eventually transforms into a new type of acoustic wave. However, the characteristics of any acoustic mode change continuously with this transformation.
The variation of film thicknesses within wide range helps to obtain a variety of *novel* materials with different combinations of characteristics demanded for SAW devices of different applications. After a proper combination of materials is selected, the geometrical parameters of a multilayered structure must be optimized to satisfy the desired electrical specification, including frequency bandwidth, insertion loss, out-of-band rejection, shape factor of frequency response or Q factor of a SAW resonator, temperature deviation of frequency etc. It is a common practice to optimize film and electrode thicknesses and other geometrical parameters of IDTs simultaneously with orientations of anisotropic materials included in the layered structure, to achieve the best SAW device performance.
The challenges described above require a robust, fast and universal numerical technique, which could be applied to different types of multilayered structures, with film thicknesses varying within wide range and allowing transformation of SAW into boundary waves, plate modes or other types of acoustic waves. Such technique is described in the next section.

3. An advanced numerical technique for analysis of acoustic waves in multilayered structures

The most popular numerical technique used for simulation of SAW characteristic in multilayered structures is *Transfer Matrix Method* (TMM) (Adler, 1990). It is based on the matrix formalism suggested by Stroh (Stroh, 1965) for solution of a SAW problem in anisotropic media. For each material of a multilayered structure, TTM assumes building of a *fundamental acoustic tensor* dependent on the material constants and the analyzed orientation. Then the characteristics of the partial acoustic modes are found as the eigen vectors and eigen values of the matrix associated with this tensor. Finally, the *transfer matrix* is calculated, which characterizes the change of acoustic fields within the analyzed layer. The method is fast and convenient and does not impose any limitations on the number of layers. However, it is known to work unstable when the film thickness exceeds 3-5 wavelength because of bad conditioned matrices built of elements, some of which exponentially decay and others exponentially grow with film thickness. These elements are associated with *incident* and *reflected* modes. As suggested by Tan (Tan, 2002) and Reinhardt (Reinhardt et al., 2003), a separate treatment of these two groups of partial modes helps to avoid the instability and extends the range of the analyzed thicknesses from zero to infinite value.

Another limitation of the previously reported numerical techniques developed for analysis of SAW in multilayered structures is their focusing on a certain type of acoustic waves, which is related to a fixed type of a multilayered structure, with analytically defined boundary conditions at the interfaces and external boundaries. For example, acoustic waves propagating in a substrate with a thin film of finite thickness and *stress-free* boundary conditions at the top surface are different from acoustic waves propagating in the same combination of materials when the film thickness tends to infinite value. In practice, the results obtained with different versions of software using fixed boundary conditions often diverge and do not allow seeing how the wave characteristics change continuously with variation of film thickness within wide range. For example, the software *FEMSDA* (Endoh et al., 1995; Hashimoto et al., 2007, 2008), which is very popular among SAW device designers, includes separate versions for analysis of SAW in a substrate with a thin film and for investigation of boundary waves. In the first version, a film thickness providing robust calculations does not exceed a half-wavelength.

To overcome the described limitation, an advanced numerical technique was developed (Naumenko, 2009, 2010). It can be applied to a variety of multilayered structures and types of acoustic waves. The universal character of the software is achieved due to characterization of the air as a dielectric medium with a very small density and elastic stiffness constants and treatment of this medium as an example of a dielectric. The same numerical methods are applied to this and other materials, which compose a layered structure. With such approach, it is not necessary to fix the stress-free boundary conditions at the top surface of a thin film or at the boundaries of a finite-thickness plate to find acoustic waves propagating in these structures. The stress-free boundary conditions are automatically simulated with high accuracy when the adjacent medium is specified as the air.

The developed technique refers to a multilayered structure schematically shown in Fig. 3, in which a metal film or IDT is located between N upper and M lower layers, where M and N can vary between one and ten or more if necessary.

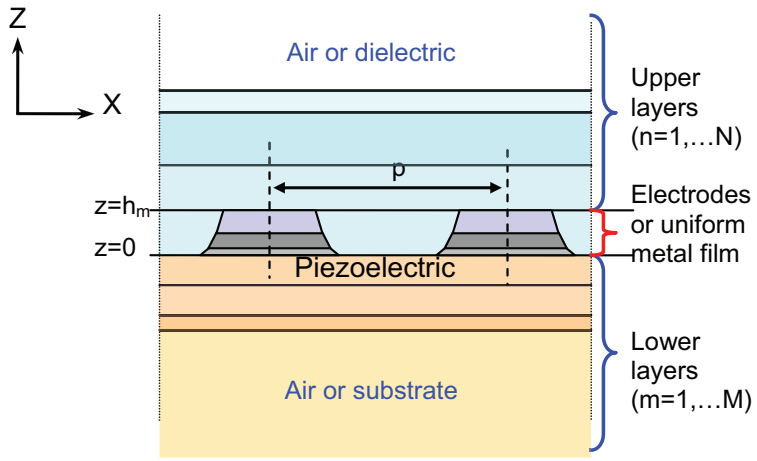

Fig. 3. Schematic drawing of analyzed multilayered structure

Analysis starts from the uppermost or lowermost half-infinite material, in which the wave structure is calculated. It can be a dielectric, a piezoelectric material or the air. In each adjacent finite-thickness layer, the transformation of the wave structure is deduced via separate treatment of incident and reflected partial modes. It means that the reflection and transmission matrix coefficients replace the transfer matrix to escape numerical noise at film thicknesses exceeding 3-5 wavelengths. For the structures with few dielectric (isotropic) films, the variation of the dielectric permittivity within each film characterized by the finite thickness h and dielectric permittivity ε_{film} is taken into account via the well known recursive equation (Ingebrigtsen, 1969):

$$\varepsilon(z+h)=\varepsilon_{film}\frac{\left[\varepsilon(z)+\varepsilon_{film}\cdot th(kh)\right]}{\left[\varepsilon_{film}+\varepsilon(z)\cdot th(kh)\right]}, \tag{1}$$

where k is the wave number. Analysis of the lower and upper multilayered half-spaces is considered completed when the wave structure has been determined at z=0 and z=h_m, where h_m is a metal film thickness, and the surface impedance matrices $\hat{Z}_{UP}(k)$ and $\hat{Z}_{LOW}(k)$ have been calculated at the upper and lower boundaries of the metal film. Each of these matrices characterizes the ratio between the vectors of displacements $\mathbf{u}$ and normal stresses $\mathbf{T}$ at the analyzed interface, $\hat{Z}=\mathbf{u}\mathbf{T}^{-1}$. A piezoelectric material is characterized by the generalized 4-dimensional displacement and stress vectors, with added electrostatic potential ϕ and normal electrical displacement D, respectively. The matrices $\hat{Z}_{UP}(k)$ and $\hat{Z}_{LOW}(k)$ comprise the information about the layers located above and below the metal film and enable simple formulation of electrical boundary conditions at z=0 and z=h_m. If the mass load of metal film is included in the analysis of the upper N layers, then the function of *effective dielectric permittivity* (EDP) $\varepsilon_s(k)$ can be calculated at z=0 (Ingebrigtsen, 1969; Milsom et al., 1977). This function relates the electric charge σ at the surface to the electrostatic potential φ,

$$\sigma = |k| \cdot \varepsilon_s(k) \cdot \varphi \tag{2}$$

and can be used for extraction of the velocities and electromechanical coupling coefficients of SAW and other acoustic modes propagating in a multilayered structure. EDP function was originally introduced for semi-infinite piezoelectric medium, but it is also an efficient tool for analysis of acoustic waves in layered structures.

The numerical method described above was extended to a periodic metal grating sandwiched between two multilayered structures. In this case, the spectral domain analysis (SDA) of the upper and lower multi-layered half-spaces is combined with the finite-element method (FEM) applied to simulation of the electrode region. To some extent, the developed *SDA-FEM-SDA* technique (Naumenko, 2010) can be considered as an advanced FEMSDA method. In this case, the function of Harmonic Admittance $Y(f,s)$ (Blotekjear et al, 1973; Zang et al, 1993) is calculated. Similar to EDP function, Harmonic Admittance relates the electric charge on the electrodes of the infinite periodic grating Q to the applied harmonically varying voltage V_e,

$$Q = (j\omega)^{-1} Y(f,s) \cdot V_e \tag{3}$$

and depends on frequency f and the normalized wave number, $s = p / \lambda$, where p is a pitch of the grating. This function can be used for simulation of a SAW resonator and calculation of its main parameters: resonant and anti-resonant frequencies, reflection coefficient etc. Also it comprises the information about SAW and other acoustic modes, which can be generated in the analyzed layered structure, and their characteristics can be extracted from $Y(f,s)$.

It should be mentioned that a numerical procedure of finding eigen modes of the fundamental acoustic tensor can be successfully applied to the air as an example of isotropic medium and the calculated SAW characteristic do not differ noticeably from that obtained with stress-free conditions set analytically at the film/air interface. The method and software SDA-FEM-SDA enable analysis of electrodes composed of few different metal layers and having a complicated profile, with different edge angles in metal layers. The gaps between electrodes may be empty or filled with a dielectric material. Due to these options, some important physical effects can be simulated, such as the effect of a sublayer (e.g. titanium) often used for better adherence of electrode metal to the substrate or the effect of nonrectangular electrode profile on a SAW device performance.

The developed numerical technique can be applied to different types of multilayered structures and different acoustic waves can be investigated, for example,

a. SAW and LSAW in a piezoelectric substrate;
b. SAW and LSAW in a substrate with one or few thin films (e.g. Love modes);
c. plate modes generated by IDT and propagating in a thin plate (e.g. Lamb waves);
d. boundary waves propagating along the interface between two half-infinite media;
e. acoustic waves propagating in a thin piezoelectric plate bonded to a thick wafer.

In addition, a continuous transformation between different types of acoustic waves can be observed. It gives a physical insight into the mechanisms of wave transformation with increasing film thickness. An example of wave transformation will be considered in Section 5.

4. Multilayered structures: examples of analysis

In this section, few examples of application of the developed numerical technique to the structures of practical importance are presented.

4.1 SiO_2/42°YX LT with Al film at the interface

The first example is a dielectric film on a piezoelectric substrate, which can be referred to the *Type 2* structure shown in Fig.1. The calculated characteristics of LSAWs propagating in SiO_2/42°YX LT with uniform Al film atop of the structure are presented in Fig. 4.

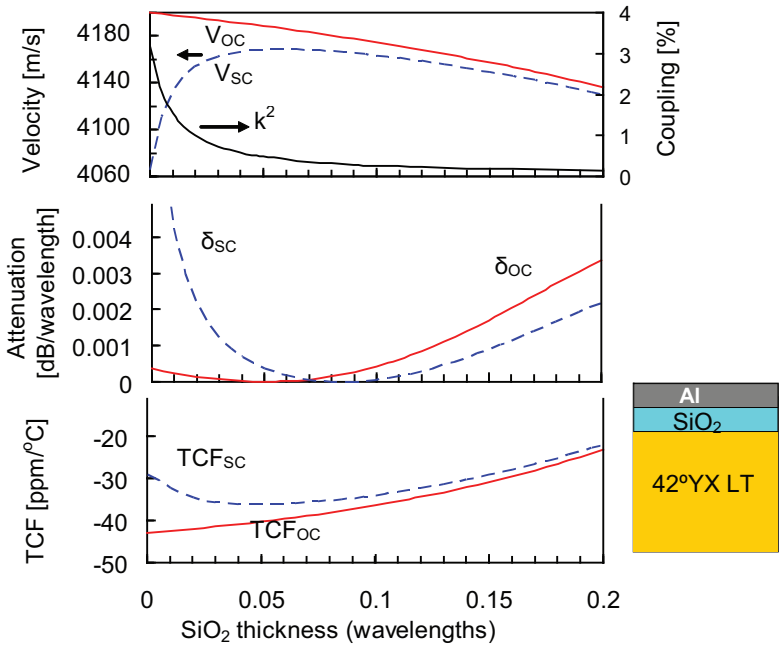

Fig. 4. Characteristics of leaky SAW propagating in SiO_2/42°YX LT with uniform Al film (h_{Al}=5%λ) atop of SiO_2 film, as functions of normalized SiO_2 film thickness. OC or SC electrical conditions are analyzed

SiO_2 is an isotropic dielectric film. LSAW velocities V, attenuation coefficients δ (in dB/λ, where λ is LSAW wavelength) and TCF are presented as functions of the normalized SiO_2 film thickness, h/λ. These characteristics have been calculated for the open-circuited (OC) and short-circuited (SC) electrical conditions in Al film. The finite thickness of a metal film (h_{Al}=5%λ) was taken into account. The difference between the OC and SC velocities determines the electromechanical coupling coefficient k^2, which decreases rapidly with increasing dielectric film thickness. The behavior of attenuation coefficients depends on the electrical condition. The functions $\delta_{OC}(h_{SiO2})$ and $\delta_{SC}(h_{SiO2})$ reach nearly zero values at h_{SiO2}=5%λ and h_{SiO2}=8%λ, respectively. Therefore, the variation of SiO_2 film thickness can be used for minimization of propagation losses in a SAW device. Due to the opposite signs of TCF in SiO_2 film and LT substrate, in the layered structure the absolute value of TCF

reduces with increasing film thickness but does not reach zero in the investigated interval of film thicknesses. However, larger SiO_2 thicknesses are not considered because the electromechanical coupling coefficient becomes too low for practical applications. Further improvement of TCF is possible if IDT is located at the SiO_2/LT interface (*Type 1* structure). Such example will be considered in Section 5.

4.2 ZnO/sapphire: existence of high-velocity SAW

The next example, ZnO film on a sapphire substrate, is a layered structure with a piezoelectric film on a non-piezoelectric substrate, which is potentially useful for high-frequency SAW device applications. Also this example demonstrates that a deposition of a thin film on a substrate can result in the existence of a high-velocity SAW, which cannot exist in a crystal without a thin film.

The typical SAW velocities in layered structures using a sapphire substrate are about 5500 m/s. Leaky SAWs, which have higher velocities, propagate with certain attenuation dependent on orientation of a substrate. Two types of LSAW can exist in crystals and layered structures: common or low-velocity LSAW, with velocities confined in the interval between that of the slow quasi-shear and fast quasi-shear *limiting* bulk acoustic waves (LBAWs), and high-velocity LSAW with velocities between that of the fast quasi-shear and quasi-longitudinal LBAWs. The *limiting* BAW is a bulk wave, which propagates in the sagittal plane (i.e. the plane, which is normal to the substrate surface and parallel to the propagation direction of SAW or LSAW) and is characterized by the group velocity parallel to the substrate surface. Usually a high velocity LSAW is not suitable for SAW device applications because of its fast attenuation. In some crystals with strong acoustic anisotropy, a high-velocity LSAW degenerates into the quasi-longitudinal LBAW in selected orientations, and low-attenuated LSAW can propagate around such orientations (Naumenko, 1996). For example, such waves exist in some orientations of quartz and LBO.

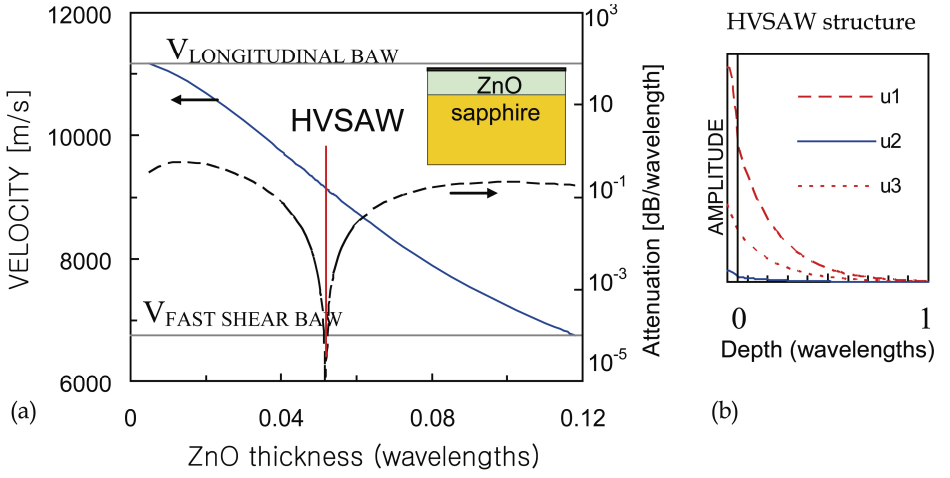

Fig. 5. (a) Velocity and attenuation coefficients of high-velocity leaky waves propagating in sapphire, Euler angles (0°, -20.3°, 0°), with ZnO film, as functions of normalized ZnO thickness, and (b) Displacements as function of depth, for HVSAW existing at h_{Zn0}=5.16%λ

Fig. 5, a shows the calculated velocities and attenuation coefficients of high-velocity LSAWs propagating in ZnO/sapphire structure, when the sapphire orientation is defined by the Euler angles (0°, -20.3°, 0°). The thickness of a metal film deposited atop of ZnO is not taken into account. The velocities of the fast quasi-shear and quasi-longitudinal LBAWs in sapphire are shown as $V_{FAST\ SHEAR\ BAW}$ and $V_{LONGITUDINAL\ BAW}$, respectively. The non-attenuated SAW solution, which occurs on a high-velocity LSAW branch at $h_{ZnO}\approx 5.16\%\lambda$ (Fig.5, a), is not a quasi-bulk wave described above. Fig.5,b shows the mechanical displacements, which follow the propagation of this wave. The analyzed solution is a sagittally polarized surface wave, which attenuates exponentially into the depth of sapphire, similar to Rayleigh SAW. Such *high velocity SAW* (HVSAW) can not exist without perturbation of a free crystal surface, e.g. by deposition of a thin film or a metal grating. The existence of this type of waves was revealed via numerical analysis of experimental data on SAW modes in ZnO/SiC structure (Didenko et al., 2000) and confirmed by other examples of layered structures, which support propagation of these waves, such as ZnO/diamond, Zno/sapphire etc. (Naumenko & Didenko, 1999).

The HVSAW found in ZnO/sapphire may be attractive for applications in high-frequency SAW devices because it combines a high propagation velocity exceeding 9000 m/s with electromechanical coupling about 0.3%. With deposition of a metal film or a periodic metal grating the wave with attractive properties does not disappear but a combination of cut angle and ZnO thickness should be optimized properly to provide low LSAW attenuation.

4.3 Al grating on 46ºYX LT/Si bonded wafer

In this example, SAW modes are investigated in LT/Si structure with a periodic Al grating atop of LT, which can be obtained experimentally by bonding LT plate to a silicon wafer. In such structure, the TCF may be dramatically reduced compared to regular LT wafer.

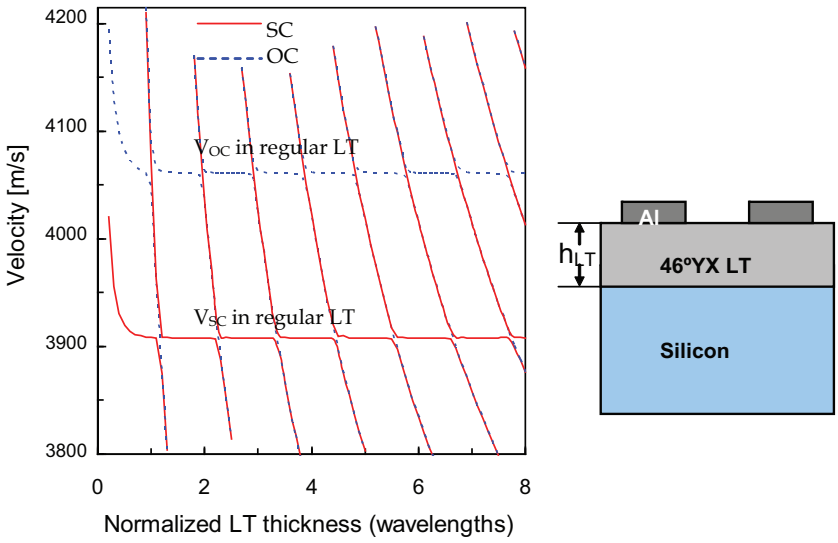

Fig. 6. Velocities of acoustic modes propagating in 46ºYX LT plate bonded to silicon wafer, with OC and SC Al grating, as functions of normalized LT thickness, h_{Al}=9%λ

The results shown in Fig.6 were obtained with the software SDA-FEM-SDA because the effect of a periodic metal grating is different from that of a uniform metal film. When LT thickness is about 1-2 wavelengths, the velocity of the SAW mode propagating in the layered structure is nearly the same as in a regular LT substrate with electrode thickness h_{Al}=9%λ but the wave characteristics are perturbed by interactions with multiple plate modes, the number of which grows with increasing LT thickness. It should be noted that in a regular 46ºYX LT substrate the acoustic wave propagating with nearly the same velocity has a leaky wave nature. The bonding of LT plate to a silicon wafer results in the transformation of LSAW into SAW. The leakage of the wave becomes impossible because in silicon the shear BAW propagates faster than the analyzed SAW mode.

4.4 Al grating on 46ºYX LT/SiO_2/Si bonded wafer

The next example differs from the previous one by the additional SiO_2 film between LT and Si wafer. A silicon dioxide layer is required to be deposited on the LT wafer to enable a stronger bond to silicon (Abbott et al., 2005). The presence of additional SiO_2 film impacts the acoustic and electrical properties of a bonded wafer and SAW resonators built on its surface. The spectrum of acoustic modes propagating in LT/SiO_2/Si bonded wafer looks more complicated than in LT/Si structure and depends on SiO_2 and LT thicknesses. In Fig. 7, the velocities of acoustic modes are shown as functions of the normalized SiO_2 film thickness when LT thickness is fixed, h_{LT}=6λ.

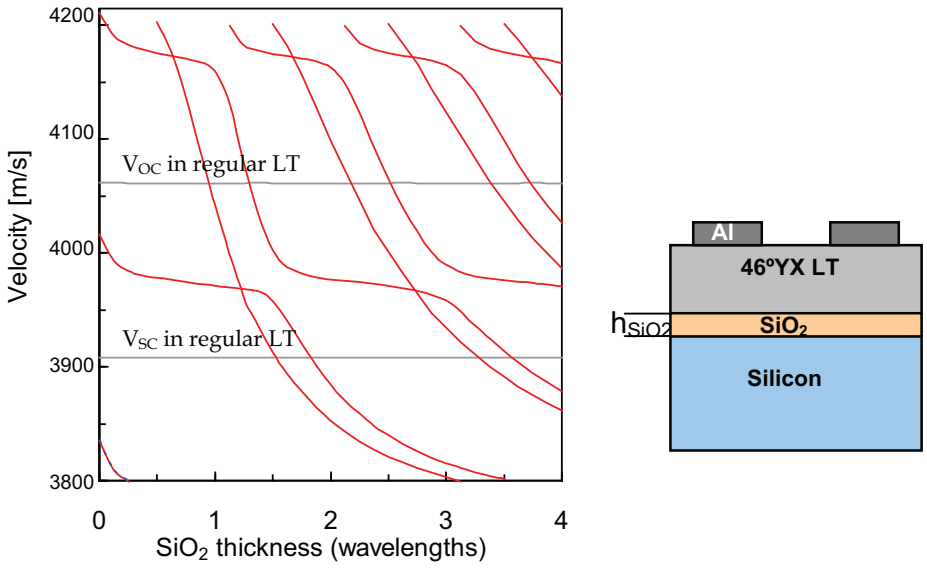

Fig. 7. Velocities of acoustic modes propagating in 46ºYX LT/SiO_2/Si structure with Al grating, as functions of normalized thickness of SiO_2 film, when h_{LT}=6λ and h_{Al}=9%λ

4.5 Cu grating buried in SiO_2, on 46ºYX LT/SiO_2/Si bonded wafer

This numerical example refers to the same bonded structure as described above but demonstrates the effect of additional SiO_2 overlay deposited over periodic metal grating

electrodes. Such layer is aimed at further improvement of the temperature characteristics of SAW devices.

In this case, Cu electrodes are investigated because this metal provides higher reflection coefficients in SAW resonators and hence lower insertion loss in RF SAW filters than Al, when electrodes are buried in SiO_2 overlay. The velocities of acoustic modes are shown in Fig.8 as functions of the normalized intermediate SiO_2 film thickness, while the thicknesses of SiO_2 overlay, LT plate and Cu electrodes are fixed, h_{OVL}=0.25%λ, h_{LT}=4λ and h_{Cu}=2.5%λ, respectively. The dispersion of SAW velocities in 46°LT/SiO_2/Si (Fig. 8,a) and SiO_2/46°LT/SiO_2/Si (Fig. 8,b) structures demonstrates that in practice very accurate simulation is required to account for all spurious modes, because these modes may affect the admittance of a SAW resonator.

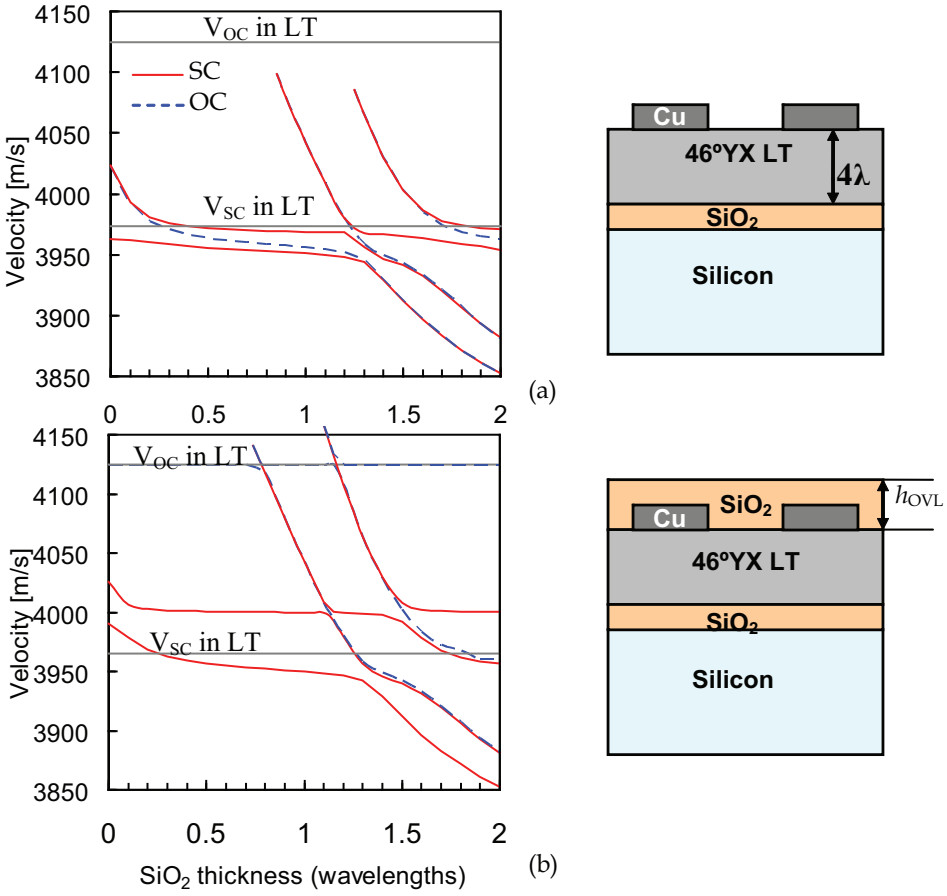

Fig. 8. Velocities of acoustic modes as functions of normalized thickness of intermediate SiO_2 film, when h_{LT}=4λ and h_{Cu}=2.5%λ, (a) in 46°LT/SiO_2/Si structure with Cu grating, and (b) in SiO_2/46°LT/SiO_2/Si structure with Cu grating atop of 46°LT plate and overlay thickness h_{OVL}=0.25%λ

Fig. 9 demonstrates an example of calculated admittance of a periodic Cu grating used with different multilayered structures described above. In addition to the main SAW mode, which exhibits resonance and anti-resonance, the multiple spurious modes propagate in the analyzed layered structures and can disturb a SAW resonator performance. The frequencies of the spurious responses are very sensitive to the thicknesses of the layers in a multilayered structure. However, the accurate simulation of these modes enables optimization of the layered structure to minimize the effect of the spurious modes on a resonator performance.

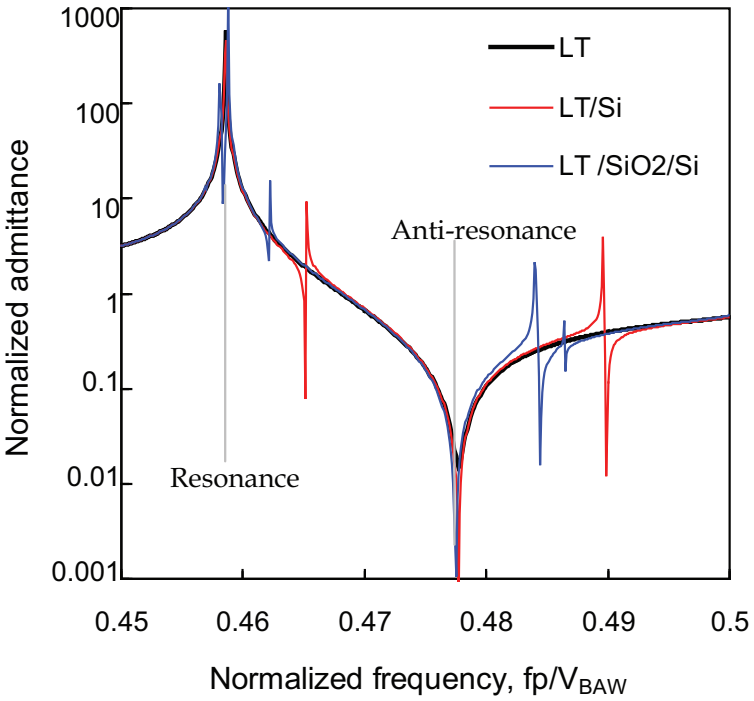

Fig. 9. Admittance of infinite periodic grating with Al electrodes (h_{Al}=10%λ), as function of normalized frequency, when the grating is built on regular 42°YX LT substrate, on LT plate (h_{LT}=5.5λ) bonded to Si substrate and atop of LT/SiO_2/Si structure, with h_{SiO2}=2λ. V_{BAW}=4214.636 m/s

The effect of spurious modes on a resonator performance can be minimized by the variation of rotation angle of LT plate. If one of rotated YX cuts of LN is used as a piezoelectric plate, the insertion loss of a resonator SAW device can be reduced in a wider bandwidth.

The examples presented in this section illustrate possible applications of the developed numerical technique and demonstrates that being a part of design tools for SAW device simulation it can be also an efficient tool for analysis of acoustic modes in multilayered structures.

5. Transformation of acoustic waves in anisotropic layered structures

In isotropic or highly symmetric materials, acoustic waves are characterized by mechanical displacements either belonging to the sagittal plane, $\boldsymbol{u}=(u_1, 0, u_3)$, or normal to this plane, $\boldsymbol{u}=(0, u_2, 0)$, i.e. such waves are Rayleigh-type or SH polarized modes. Similar solutions occur in some symmetric orientations of materials belonging to the lower symmetry classes. Such solutions have been extensively studied analytically. To the best author's knowledge, the most comprehensive overview of different types of acoustic waves existing in substrates with thin films, in thin plates and at the boundary between two half-infinite media was made by Viktorov (Viktorov, 1967, 1981). Some statements, which refer to acoustic waves propagating in isotropic structures, are listed below.

a. In isotropic substrate with isotropic thin film, SH-polarized Love waves can propagate if the shear BAW propagates faster in a substrate than in a film.
b. Along the boundary between two rigidly connected isotropic half-infinite media, the sagittally polarized Stonely waves can propagate. These waves are usually trapped near the interface between two media, with penetration depth about one wavelength.
c. SH-polarized boundary waves can exist if additional thin film with lower shear BAW velocity is added between two half-infinite media.
d. In isotropic thin plates, two types of waves can exist: sagittaly polarized Lamb waves (symmetric and anti-symmetric modes) and SH-polarized plate modes. With increasing plate thickness, higher-order modes appear and their number increases.
e. With plate thickness decreasing to zero, the first-order symmetric Lamb mode degenerates into the longitudinal BAW. With increasing plate thickness, this mode finally degenerates into two Rayleigh SAWs propagating along the boundaries of the plate.
f. Higher-order plate modes arise from the shear and longitudinal BAWs at certain cut-off thicknesses and have a structure of standing waves propagating between two interfaces.

The layered structures used in SAW devices must include at least one anisotropic material to provide a piezoelectric coupling of SAW with IDT. Anisotropy results in mixed polarizations of acoustic modes propagating in thin films, plates and along the interface between two media. The transformation of each mode with increasing film thickness is unique and requires separate investigation. Whereas analytical study of such waves is possible only in some symmetric orientations, the numerical technique presented in this chapter enables calculation of the wave characteristics and analysis of displacements associated with different acoustic modes. Its application to multilayered structures can reveal the mechanisms of wave transformation. The understanding of these mechanisms helps to select properly the thicknesses of metal and dielectric or piezoelectric layers to ensure the propagation of a required acoustic wave.

An example of such investigation is presented here. It refers to 42°YX LT with SiO_2 film. Similar structure was considered in Section 4.1, but in the present example a periodic grating is analyzed instead of a thin metal film and this grating is located at the interface between LT substrate and SiO_2 film. As a metal of the grating, copper is considered. Such structure is of great practical importance as potential material for RF SAW devices with improved temperature characteristics.

The calculated velocities of acoustic modes propagating in LT substrate with copper grating are shown in Fig.10,a as functions of the Cu electrode thickness. Fig.10,b shows the velocities

of acoustic waves propagating in SiO_2/Cu grating/LT structure, as functions of the normalized SiO_2 thickness, with Cu thickness fixed, h_{Cu}=0.2λ. The analyzed Cu thicknesses look too high for application in SAW resonators but provide better insight into the wave transformation mechanisms, which is a purpose of this investigation.
When the metal thickness is small, two acoustic waves exist in LT, SAW1 and LSAW. With increasing Cu thickness, the velocities of both modes decrease rapidly and at h_{Cu}=0.075λ LSAW transforms into the second SAW mode, SAW2. With further increasing of electrode thickness, two SAW modes interact with each other. To avoid discontinuities in the characteristics of two SAW modes, these modes are distinguished by their velocities: $V_{SAW2}>V_{SAW1}$.

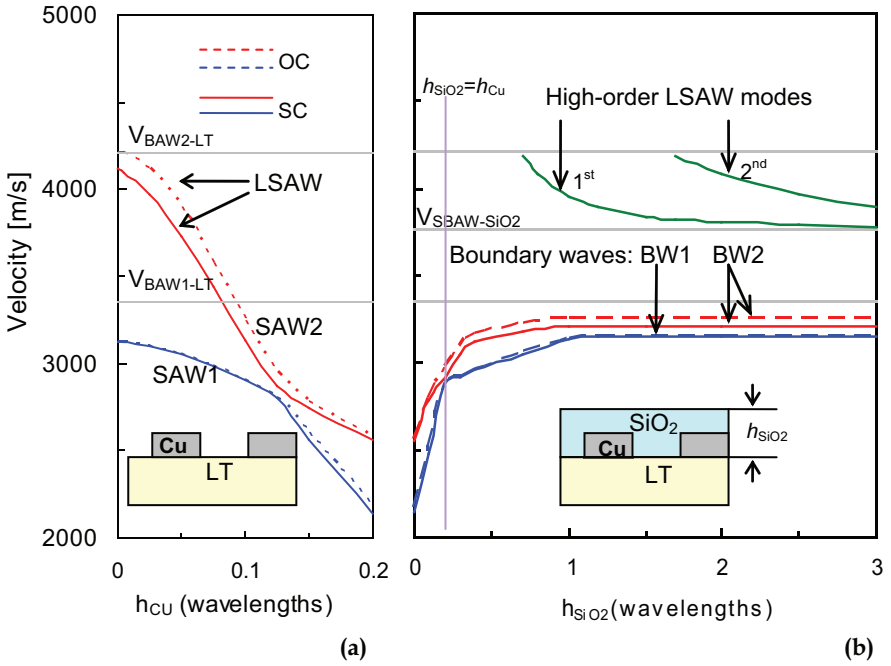

Fig. 10. SAW and leaky SAW velocities in 42°YX LT, (a) with Cu film, as functions of film thickness; (b) with Cu and SiO_2 films, as functions of normalized SiO_2 film thickness

If metal thickness is fixed (h_{Cu}=0.2λ) and the gaps between electrodes are filled with SiO_2, the velocities of two SAW modes grow rapidly (Fig.10,b). Another interaction between SAW1 and SAW2 occurs at $h_{SiO2}\approx h_{Cu}$, i.e. when the top surface of the whole structure becomes flat. With increasing SiO_2 film thickness two SAW modes finally transform into the boundary waves, BW1 and BW2. The boundary waves propagate with velocities lower than that of the shear BAW in SiO_2. The wave BW2 shows electromechanical coupling sufficient for application in resonator SAW devices, k^2=3.49%. For this mode, TCF grows from -31 ppm/°C in LT substrate up to 10 ppm/°C in a layered structure with SC grating and from -43 ppm/°C up to 6 ppm/°C with OC grating. At h_{SiO2}>0.7λ, higher-order plate modes arise from the fast shear limiting BAW in LT.

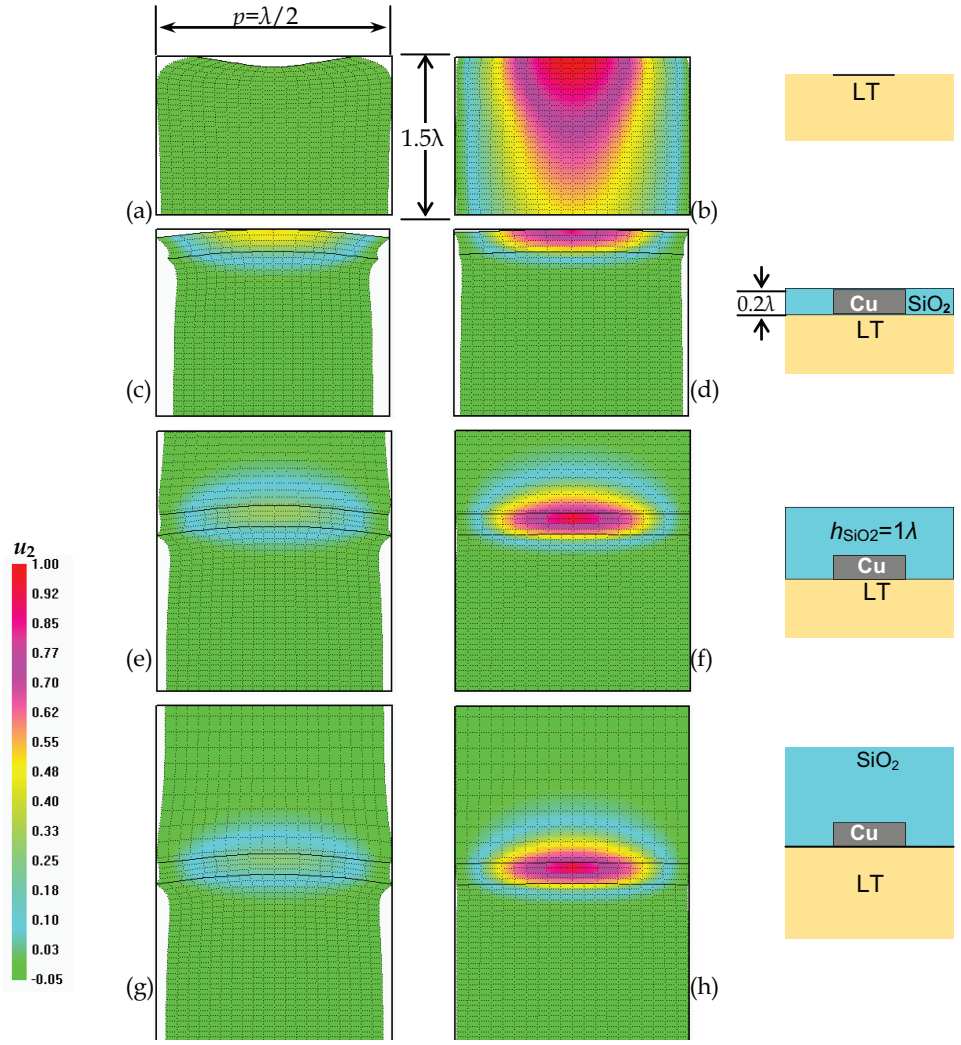

Fig. 11. Transformation of two SAW modes in 42°YX LT with Cu grating with increasing SiO_2 film thickness; (a), (c), (e), (g) SAW1, (b), (d), (f), (h) SAW2

Fig.11 demonstrates how the acoustic fields associated with the modes SAW1 and SAW2 change with increasing SiO_2 film thickness. OC electrical condition is considered, by way of example. The components of mechanical displacements in the sagittal plane are revealed as perturbations of the regular mesh and the values of SH components are presented as colored diagrams. When Cu thickness is small (Fig.11,a,b), SAW1 is nearly perfect Rayleigh wave and LSAW is a quasi-bulk SH-type wave slowly attenuating with depth. When $h_{Cu}>0.075\lambda$, LSAW transforms into SAW2, which is also SH-type wave. At Cu thicknesses about 0.12λ, both SAW modes are perturbed by interaction between them. In the interval of

Cu thicknesses between 0.12λ and 0.2λ, the modes SAW1 and SAW2, which have been determined as the lower-velocity and higher velocity modes, exchange their polarizations. After the second interaction, which occurs at $h_{SiO2}=h_{Cu}=0.2\lambda$, SAW1 and SAW2 turn back into Rayleigh-type and SH-type waves, respectively. However, at $h_{Cu}=0.2\lambda$ (Fig.11,c,d) both waves still have mixed polarizations. With increasing SiO_2 film thickness, SAW1 and SAW2 transform into the boundary waves BW1 and BW2, respectively (Fig. 11, g, h), with acoustic waves localized in Cu grating and around it. The boundary waves have mixed polarizations, which would be impossible in isotropic substrate with isotropic thin film, but due to specific features of the analyzed LT orientation, BW1 is nearly sagittally polarized wave and BW2 is nearly pure SH wave. BW2 penetrates deeper into SiO_2 film than into LT substrate. A numerical analysis reveals that SiO_2 thickness about 1.5λ is sufficient for transformation of SAW into the boundary wave.

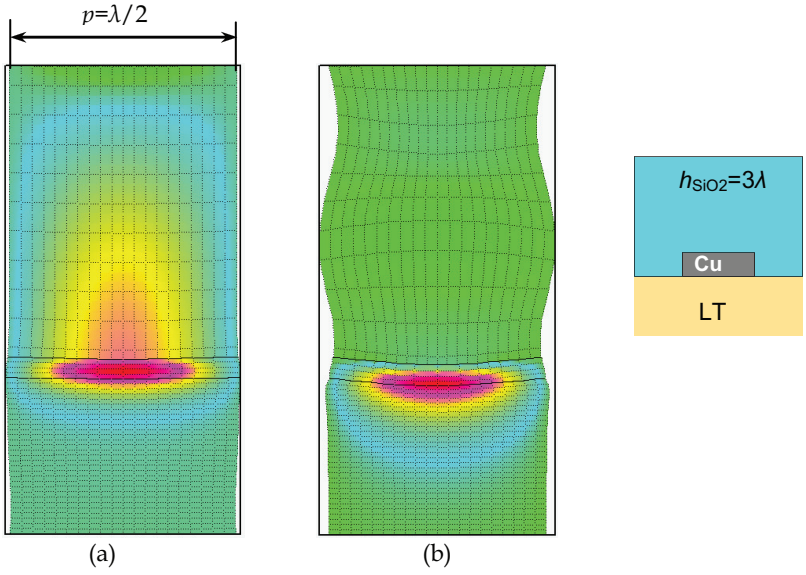

Fig. 12. Acoustic fields associated with two higher-order modes propagating in 42°YX LT with Cu grating and SiO_2 film when $h_{SiO2}=3\lambda$. (a) 1st mode; (b) 2nd mode

The acoustic fields associated with propagation of the two higher-order modes (Fig.10,b) have been also investigated. These modes have leaky wave nature. Fig.12 illustrates the structure of these modes at $h_{SiO2}=3\lambda$. The first mode, which exists when $h_{SiO2}>0.7\lambda$, has SH polarization deeply penetrating into SiO_2 (Fig.12,a). With increasing SiO_2 thickness, this mode degenerates into the SH BAW propagating in SiO_2. The second mode, which exists at $h_{SiO2}>1.6\lambda$, looks as a combination of SH-type SAW in LT substrate with Cu grating and sagittally polarized quasi-bulk wave propagating in SiO_2 (Fig.12,b), with the amplitude of SH polarization component much higher than the amplitudes of two other components. This example demonstrates the effect of anisotropy on the propagation of acoustic waves in

multilayered structures and reveals another application of the numerical technique described in this chapter. Similar investigation can be performed for other structures of practical importance or serve to study the wave processes in multilayered structures.

6. Conclusion

In this chapter, some layered and multilayered structures, which look promising as substrates for modern SAW devices developed for applications in cellular phones, communication and navigation systems have been overviewed. A universal numerical technique, which enables fast and accurate analysis of these and other structures have been presented and, by way of example, applied to some multilayered structures of practical interest. The physical insight into the mechanisms of SAW transformation with increasing film thickness in a multilayered structure was provided via simulation of acoustic fields in one of the structures.

7. References

Abbott B.P., Naumenko N.F. & Caron J. (2005). Characterization of bonded wafer for RF filters with reduced TCF, *Proceedings of IEEE Ultrasonics Symposium*, pp.926-929, Rotterdam, the Netherlands, Sept. 2005.

Adler E. L. (1990). Matrix methods applied to acoustic waves in multi-layers, *IEEE Trans. Ultrason., Ferroelectr., Freq. Control*, Vol. 37, No 6, pp. 485-490.

Ballandras S., Reinhardt A., Laude L., Soufyane A., Camou S. & Ventura P. (2004). Simulations of surface acoustic wave devices built on stratified media using mixed finite element/boundary integral formulation, *J. Appl. Phys.*, Vol. 96, No 12, pp.7731-7741.

Benetti M., Cannatta D., Pietrantonio F. D. & Verona E. (2005). Growth of AlN piezoelectric film on diamond for high-frequency surface acoustic wave devices, *IEEE Trans. Ultrason., Ferroelectr., Freq. Control,* Vol. 52 , pp. 1806–1811.

Benetti M., Cannata D., Di Pietrantonio F., Verona E., Almaviva S., Prestopino G., Verona C. & Verona-Rinati G. (2008). Surface acoustic wave devices on AlN/single-crystal diamond for high frequency and high performances operation, *Proceedings of IEEE Ultrasonics Symposium,* pp. 1924-1927, Beijing, China, Nov. 2008.

Blotekjear K., Ingebrigsten K. & Skeie H. (1973). A method for analyzing waves in structures consisting of metal strips on dispersive media, *IEEE Trans. Electronic Devices*, vol. 20, no. 12, pp. 1133–1138.

Brizoual L. L., Sarry F. , Elmazria O. , Alnot P. , Ballandras S. & Pastureaud T. (2008). GHz frequency ZnO/Si SAW device, *IEEE Trans. Ultrason., Ferroelectr., Freq. Control*, Vol. 55, No 2, pp. 442–450.

Didenko I. S., Hickernell F. S. & Naumenko N. F. (2000). The theoretical and experimental characterization of the SAW propagation properties for zinc oxide films on silicon carbide, *IEEE Trans. Ultrason., Ferroelectr., Freq. Control*, Vol. 47, No. 1, pp.179-187.

Eda K., Onishi K., Sato H., Taguchi Y. & Tomita M. (2000). Direct bonding of piezoelectric materials and its applications, *Proceedings of IEEE Ultrasonics Symposium* , pp. 299-309, San Juan, Puerto Rico, Sep. 2000.

Emanetoglu N.W., Patounakis G., Muthukumar S. & Lu Y. (2000). Analysis of temperature compensated modes in ZnO/SiO_2/Si multilayer structures, *Proceedings of IEEE Ultrasonics Symposium* , pp. 325-328, San Juan, Puerto Rico, Sep. 2000.

Endoh G., Hashimoto K. & Yamagouchi M. (1995). SAW propagation characteristics by Finite Element Method and Spectral Domain Analysis, *Jpn. J. Appl. Phys*., Vol. 34, No 5B, pp. 2638-2641.

Fujii S., Kawano S., Umeda T., Fujioka M. & Yoda M. (2008). Development of a 6GHz resonator by using an AlN diamond structure, *Proceedings of IEEE Ultrasonics Symposium*, pp. 1916-1919, Beijing, China, Nov. 2008.

Hashimoto, K. Y. (2000). *Surface Acoustic Wave Devices in Telecommunications: Modeling and Simulation*, Springer, ISBN 354067232X, USA.

Hashimoto K., Omori T. & Yamaguchi M. (2007). Extended FEM/SDA Software for Characterizing Surface Acoustic Wave Propagation in Multi-layered Structures, *Proceedings of IEEE Ultrasonics Symposium*, pp. 711-714, Rome, Italy, Nov. 2008.

Hashimoto K., Wang Y., Omori T., Yamaguchi M., Kadota M., Kando H. & Shibahara T. (2008). Piezoelectric Boundary Waves: Their Underlying Physics and Applications, *Proceedings of IEEE Ultrasonics Symposium*, pp. 999-1005, New York, USA, Oct. 2007.

Ingebrigtsen K.A. (1969). Surface waves in piezoelectrics, *J. Appl. Phys.,* Vol. 40, No 7, pp.2681-2686.

Kadota M. & Minakata M. (1998). Piezoelectric Properties of ZnO Films on a Sapphire Substrate Deposited by an RF-Magnetron-Mode ECR Sputtering System, *Jpn. J. Appl. Phys*., Vol.37, pp.2923-2926.

Kadota M. (2007). High Performance and Miniature Surface Acoustic Wave Devices with Excellent Temperature Stability Using High Density Metal Electrodes, *Proceedings of IEEE Ultrasonics Symposium*, pp.496-506, New York, USA, Oct. 2007.

Kadota M., Nakao T., Murata T. & Matsuda K. (2008). Surface Acoustic Wave Filter in High Frequency Range with Narrow Bandwidth and Excellent Temperature Property, *Proceedings of IEEE Ultrasonics Symposium*, pp. 1584-1587, Beijing, China, Nov. 2008.

Kovacs G., Ruile W., Jakob M., Rosler U., Maier E., Knauer U. & Zottl H. (2004). A SAW Duplexer with Superior Temperature Characteristics for US-PCS, *Proceedings of IEEE Ultrasonics Symposium*, pp. 974-977, Montreal, Canada, Aug. 2004.

Milsom R. F., Reilly N.C.H. & Redwood M. (1977). Analysis of generation and detection of surface and bulk acoustic waves by interdigital transducers, *IEEE Trans. Sonics and Ultrasonics*, Vol. 24, pp. 147-166.

Nakahata H., Higaki K., Fujii S. , Hachigo A., Kitabayashi H. , Tanabe K., Seki Y. & Shikata S. (1995). SAW Devices on Diamond, *Proceedings of IEEE Ultrasonics Symposium,* pp.361-370, Seattle, USA, Nov. 1995.

Nakahata H., Hachigo A., Itakura K., Fujii S. & Shikata S. (2000). SAW Resonators on SiO_2/ZnO/Diamond Structure in GHz Range, *Proceedings of IEEE Freq. Contr. Symposium*, pp. 315-320, Kansas City, USA, June 2000.

Nakai Y., Nakao T. , Nishiyama K. & Kadota M. (2008). Surface Acoustic Wave Duplexer composed of SiO_2 film with Convex and Concave on Cu-electrodes/LiNbO3 Structure, *Proceedings of IEEE Ultrasonics Symposium*, pp.1580-1583, Beijing, China, Nov. 2008.

Nakanishi H., Nakamura H. , Hamaoka Y., Kamiguchi H. & Iwasaki Y. (2008). Small-sized SAW Duplexers with Wide Duplex Gap on a SiO_2/Al/$LiNbO_3$ structure by using Novel Rayleigh-mode Spurious Suppression Technique, *Proceedings of IEEE Ultrasonics Symposium*, pp. 1588-1591, Beijing, China, Nov. 2008.

Naumenko N. F. (1996). Application of exceptional wave theory to materials used in surface acoustic wave devices", *J. Appl. Phys.*, Vol.79, pp. 8936-8943.

Naumenko N.F. & Didenko I.S. (1999). High-velocity surface acoustic waves in diamond and sapphire with zinc oxide film, *Appl. Phys. Lett.*, Vol. 75, No 19, pp. 3029-3031.

Naumenko N.F. & Abbott B.P. (2003). Surface Acoustic Wave Devices Using Optimized Cuts of a Piezoelectric substrate, *US Patent #6,556,104 B2.* Int.Cl. H03H 9/64. Apr.29, 2003

Naumenko N.F. & Abbott B.P. (2004). Surface Acoustic Wave Filter , *US Patent 6,833,774 B2.* Int.Cl. H03H 9/16. Dec. 21, 2004.

Naumenko N.F. (2009). Transformation of Surface Acoustic Waves into Boundary Waves in Piezoelectric/Metal/Dielectric Structures, *Proceedings of IEEE Ultrasonics Symposium*, pp.2635-2638, Rome, Italy, Sep. 2009.

Naumenko N.F. (2010). A Universal Technique for Analysis of Acoustic Waves in Periodic Grating Sandwiched Between Multi-Layered Structures and Its Application to Different Types of Waves, *Proceedings of IEEE Ultrasonics Symposium*, San Diego, USA, Oct. 2010.

Naumenko N.F. & Abbott B.P. (2010). Insight into the Wave Transformation Mechanisms via Numerical Simulation of Acoustic Fields in Piezoelectric/Metal Grating/ Dielectric Structures, *Proceedings of IEEE Ultrasonics Symposium*, San Diego, USA, Oct. 2010.

Omori T., Kobayashi A., Takagi Y., Hashimoto K. & Yamaguchi M. (2008). Fabrication of SHF range SAW devices on AlN/Diamond-substrate, *Proceedings of IEEE Ultrasonics Symposium*, pp. 196-200, Beijing, China, Nov. 2008.

Reinhardt A., Pastureaud T., Ballandras S. & Laude L. (2003). Scattering matrix method for modeling acoustic waves in piezoelectric, fluid, and metallic multilayers, *J. Appl. Phys.*, Vol. 94, No 10, pp.6923-6931.

Ruppel C.C.W. & Fjeldy T. A. Eds. (2001). *Advances in Surface Acoustic Wave Technology, Systems and Applications. Volume 2* . ISBN 981-02-4538-6. World Scientific Publishing Co. Pte Ltd, Singapore.

Ruppel, C. C. W., Reindl, L. & Weigel, R. (2002). SAW devices and their wireless communication applications, *IEEE Microwave Magazine, ISSN 1527-3342* 3(2): pp. 65–71.

Stroh A. N. (1962). Steady state problems in anisotropic elasticity, *J. Math. Phys.* Vol. 41., pp. 77-103.

Tan E. L. (2002). A robust formulation of SAW Green's functions for arbitrarily thick multilayeres at high frequencies, *IEEE Trans.Ultrason., Ferroelectr., Freq. Control*, Vol. 49, No 7, pp. 929-936.

Tsutsumi J. , Inoue S., Iwamoto Y., Miura M., Matsuda T., Satoh Y., Nishizawa T., Ueda M. & Ikata O. (2004). A Miniaturized 3x3-mm SAW Antenna Duplexer for the US-PCS band with Temperature-Compensated $LiTaO_3$/Sapphire Substrate, *Proceedings of IEEE Ultrasonics Symposium*, pp. 954-958, Montreal, Canada, Aug. 2004.

Viktorov, I.A. (1967). *Rayleigh and Lamb Waves: physical theory and applications*. Plenum Press, New York.

Viktorov I.A. (1981). *Surface sound waves in solids*. Moscow: Nauka (in Russian).

Zhang Y., Desbois J. & Boyer L. (1993). Characteristic parameters of surface acoustic waves in a periodic metal grating on a piezoelectric substrate, *IEEE Trans.Ultrason., Ferroelectr., Freq. Control*, vol. 40, pp. 183-192, May 1993.